

# Melt Flow and Fiber Properties of Copolyesters

ZHANG HONG, *Department of Polymer Engineering, Beijing College of Chemical Fiber*, and LI SHENGPING and LUO HONGLIE, *Department of Polymer Science and Materials, Chengdu University of Science and Technology, People's Republic of China*

## Synopsis

The effect of modifying monomer [sodium 3,5-di(carbonethoxy)benzene sulfonate] contents range from 1.5 to 4.5 mol % on the melt flow and fiber properties of copolyesters (COPET) dyeable with basic dyes was investigated. An Instron capillary rheometer was used to obtain data over shear rates ranging from 10 to  $10^4$  s<sup>-1</sup> at 265, 275, and 285°C. The COPET's flow properties as a function of temperature, inherent viscosity, melting point, and modifying monomer content were determined. The drawn fibers annealed in oil and air at 80, 110, 130, 150, 175, and 200°C were studied by means of measurements of shrinkage ratio, crystallinity, birefringence, long period, sonic rate, and static state flexibility of molecular chain. All these showed that the large side group, —SO<sub>3</sub>Na, in COPET molecular chains causes an increase in chain rigidity and melt viscosity, and a decrease in crystallinity and orientation.

## INTRODUCTION

The base-dyeable COPET fiber can give its fabric with a high color depth and various beautiful colors and it is a copolyester of ethylene glycol, di-Me terephthalate, and Na di-Me 5—sulfoisophthalate. Since it was polymerized, much of the work has been done about the effect of modifying monomers on dyeable properties.<sup>1</sup> But compared with the detail work of poly(ethylene terephthalate) (PET),<sup>2-6</sup> little has been known about the melt flow and fiber properties and during the processing of COPET fiber, we also found that the melt viscosity increased and the extrusion was difficult. In order to understand this, in this paper, flow curves were plotted for COPET melts in terms of logarithm shear stress ( $\tau_w$ ) vs. logarithm shear rate ( $\dot{\gamma}_w$ ) over a range of inherent viscosities of COPET from 0.448 to 0.652 dL/g and modifying monomer contents from 1.5 to 4.5 mol %. Also relationships between annealing temperature and fiber crystallinity, residual extension ratio and orientation function, shrinkage ratio and long period, and shrinkage ratio and small angle X-ray scattering intensity of COPET fibers were described. The dilute solution of COPET was studied by small angle X-ray scattering to understand the chain rigidity.

## EXPERIMENTAL

### Materials

Three types of materials were used in this study: (1) copolyester of ethylene glycol, di-Mi terephthalate, and Na di-Me 5—sulfoisophthalate (*m*-COPET), supplied by Tianjing Institute of Chemical Fiber; (2) the copolyester of

TABLE I  
Characterization of COPET and PET

Polymer	<i>m</i> -COPET-1	<i>m</i> -COPET-2	<i>m</i> -COPET-3	<i>m</i> -COPET-4	<i>m</i> -COPET-5	<i>P</i> -COPET	PET
Modifying monomer contents (mol %)	1.5	2.0	2.5	3.5	4.5	3.0	—
IV (dL/g)	0.617	0.606	0.584	0.578 <sup>a</sup>	0.448	0.599	0.652
Melting point (°C)	263	252	259	255	259	248	264
COOH (eq/10 <sup>b</sup> g)	70.84	61.99	71.65	75.67	86.94	69.23	33.81
Di-glycol (%)	1.2	5.4	3.8	4.2	1.8	8.4	1.1

ethylene glycol, di-Me terephthalate, and Na di-Me 2-sulfoterephthalate (*p*-COPET), supplied by Suzhou Factory of Chemical Fiber; and (3) polyester (PET), supplied by Yiansan Co. of Oil and Chemical Engineering, Beijing. The properties of COPET and PET chips as received are listed in Table I.

### Equipment

The flow properties of seven melts were obtained with a Model 3211 Instron Capillary Rheometer in a temperature error  $\pm 1^\circ\text{C}$ . A diameter of 0.03 in. (0.762 mm) and a length to diameter ratio of 100 was selected. An Instron tensile testing machine with an isothermal chamber was used for hot air drawing.

### Procedure and Measurement

Chips were dried under the vacuum ( $< 0.6$  mm Hg) for 20 h at  $140^\circ\text{C}$  in order to minimize hydrolytic degradation during melt extrusion. Dried chips were allowed to melt for 5 min in the rheometer before testing. Fiber samples were taken at  $25^\circ\text{C}$  without drawing. A PC-1500 computer was used to calculate shear stresses and shear rates.

The low orientation fibers were uniaxially drawn to ratios of 4–6 in the testing machine at  $75^\circ\text{C}$ , drawing speed 300 mm/min. Drawing ratios were determined by the ratios of final lengths ( $L$ ) to initial lengths ( $L_0$ ).

Two types of annealing procedures were used: (1) fibers drawn to  $4\times$  and  $6\times$ , in a wire mesh basket, were immersed in silicone oil for 1 min at 80, 110, 130, 150, 175, and  $200^\circ\text{C}$ , and then quenched into carbon tetrachloride at room temperature, and (2) fibers drawn to  $6\times$ , in a wire mesh plate, were heated in air for 10 min at the same temperatures, and then cooled down to room temperature. The shrinkage ratio was calculated from the length of shranked fiber ( $L'$ ) and drawn fiber ( $L$ ) using the expression

$$S = \frac{L - L'}{L}$$

The residual extension ratio ( $\lambda'$ ) was given by the equation

$$\lambda' = \frac{L'}{L_0} = \frac{L(1 - S)}{L_0} = \lambda(1 - S)$$

Inherent viscosity was measured in phenol/tetrachloroethane (1/1 weight) with different concentrations range from 0.1 to 0.5 g/dL at  $25.0^\circ\text{C}$ . The fluctuation of temperature of water bath was controlled by an electronic relay within  $\pm 0.01^\circ\text{C}$ . Huggins' and Kraemer's equations were used for the viscosity calculation:

$$\frac{\eta_{sp}}{C} = [\eta] + K'[\eta]^2C$$

$$\frac{\ln \eta_r}{C} = [\eta] + B[\eta]^2C$$

where  $K'$  and  $B$  are constants,  $\eta_{sp}$  is the supplemental viscosity,  $\eta_r$ , the relative viscosity, and  $C$  the solution concentration. Multiple linear regression was used to determine the  $K'$ ,  $B$ , and inherent viscosity  $[\eta]$ .

Crystallinity was measured with a Model 2037 X-ray diffractometer. It was also used to obtain crystalline orientation data by azimuthal scanning on (010) and (100) planes.<sup>7</sup> The orientation function ( $f_c$ ) was given by

$$f_c = (3 \overline{\cos^2 \varphi} - 1)/2$$

$$\overline{\cos^2 \varphi}_{c,z} = 1 - \overline{\cos^2 \varphi}_{(010)} - \overline{\cos^2 \varphi}_{(100)}$$

$$\overline{\cos^2 \varphi}_{(hkl)} = \int_0^{\pi/2} I(\varphi) \cos^2 \varphi \sin \varphi \, d\varphi / \int_0^{\pi/2} I(\varphi) \sin \varphi \, d\varphi$$

where  $I(\varphi)$  is the diffracting intensity and  $\varphi_{sz}$  is an angle between the molecular chain and fiber axis.

Small-angle X-ray data of fibers and diluted solutions were also obtained from this diffractometer. The long period ( $L$ ) was determined from scattering angle ( $\theta$ ) under the maximum intensity by

$$L = \lambda/2 \sin \theta$$

where  $\lambda$  is the wavelength of the X-ray. The persistence length of molecular chain ( $L_p$ ), which was used to calculate the chain flexibility, was given by the Kratky equation<sup>8</sup>

$$L_p = \frac{2.3\lambda}{4\pi\theta_p}$$

where  $\theta_p$  is the transition point of extrapolation of two straight lines in a direction to their transition zone in the intensity curve.

## RESULTS AND DISCUSSION

### Flow Curves

The flow curves of COPET melts and PET melts were plotted at 265, 275, and 285°C. The common flow equation for stress ( $\tau_w$ ) to shear rate ( $\dot{\gamma}_w$ ) fits the data well:

$$\tau_w = K \dot{\gamma}_w^n$$

A typical kind of these flow curves for COPET melts with a 2.5 mol % modifying monomer content is shown in Figure 1. The parallelism (similar shape) of curves naturally suggests a superposition. A flow curve at one temperature was arbitrarily chosen as the reference curve. The temperature shift factor ( $a_T$ ), was the ratio of the shear rate for the reference curve to the shear rate for each of other curves at a constant shear stress. In this study the

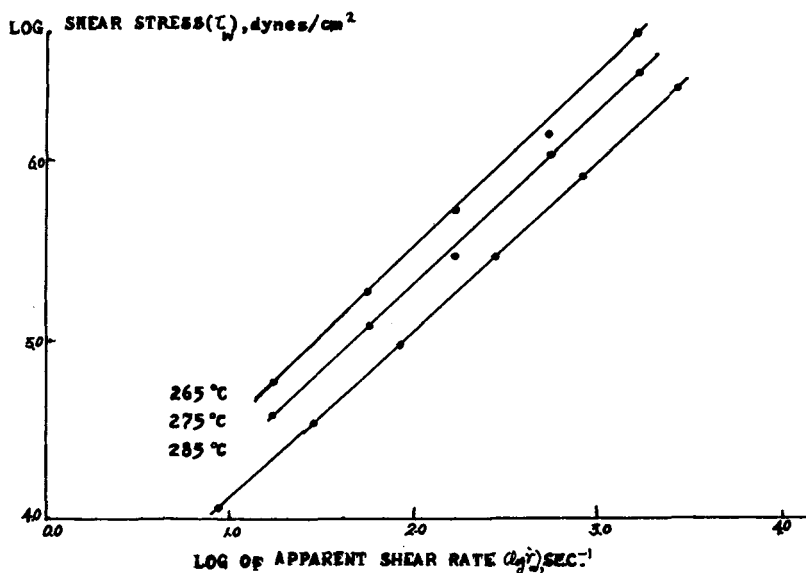


Fig. 1. Flow curves for COPET of 2.5 mol % modifying monomer.

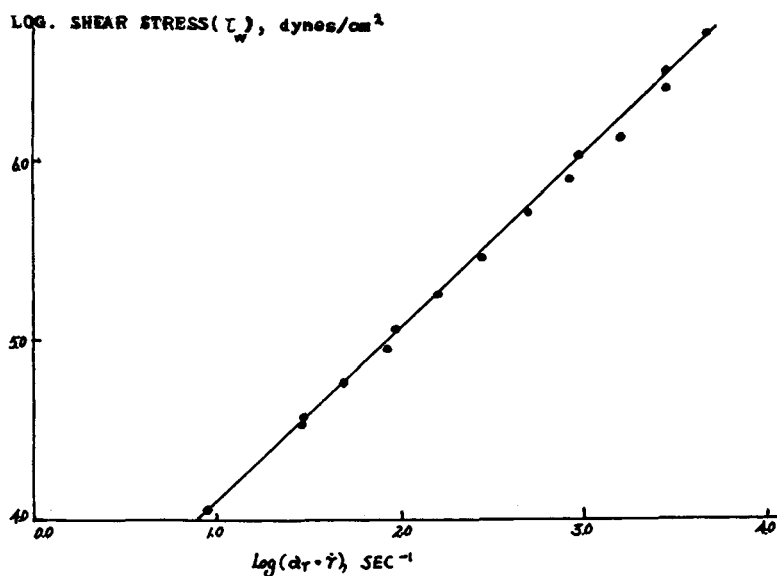


Fig. 2. Master flow curve (superposition of temperature) for COPET of 2.5 mol % modifying monomer.

flow curve at 285°C was chosen as the reference curve. The master curve thus obtained from  $\log \tau_w$  and  $\log a_T \dot{\gamma}_w$  is presented in Figure 2. The technique of temperature superposition was obviously successful. The logarithm value of the temperature shift factor  $a_T$  is a linear function of reciprocal absolute temperatures, as shown in Figure 3. That is

$$\ln a_T = -2.903 \times 10^{-3} + 1.620/T$$

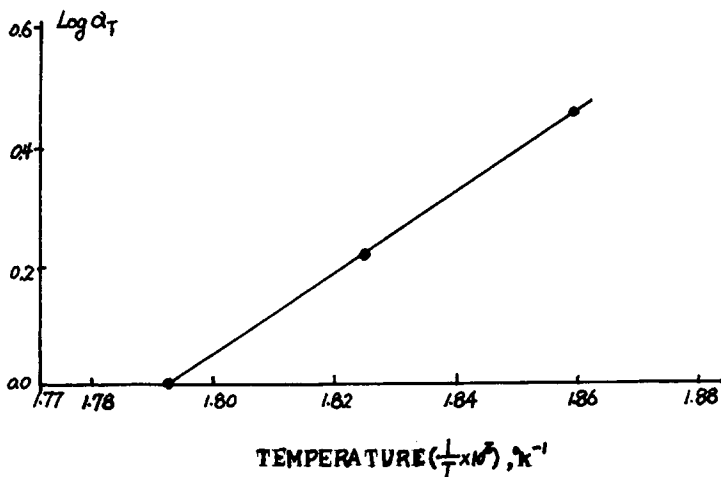


Fig. 3. Log of temperature shift factor as a function of reciprocal absolute temperature (curve of 2.5 mol % modifying monomer). Reference temperature, 285°C.

It is as same as the sample Arrhenius-type equation

$$\ln \eta = \ln A + E/RT$$

where  $\eta$  is melt viscosity,  $A$  and  $R$  are constants, and  $E$  is the viscous flow activation energy.  $E$  was calculated by comparison with the two equations. This relationship holds for COPET of all modifying monomer contents in this study. Viscous flow activation energies for COPET of modifying monomer 2.0,

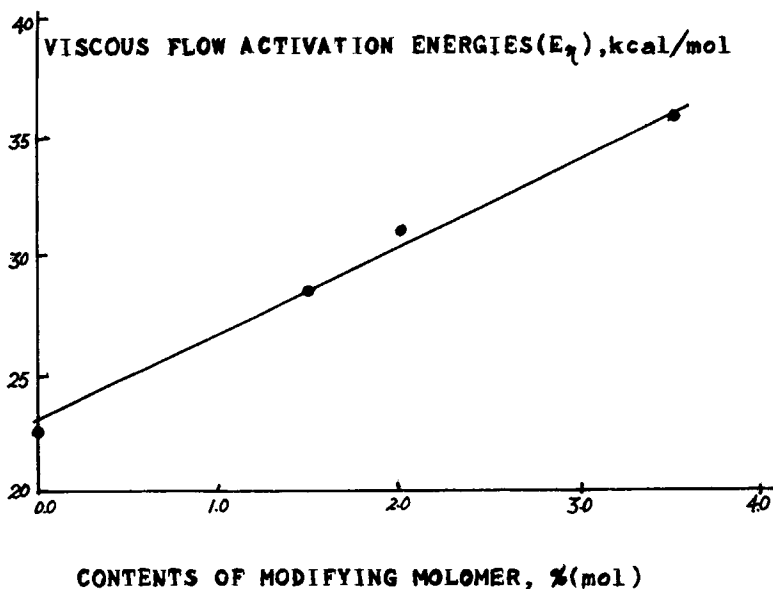


Fig. 4. Viscous flow activation energy as a function of contents of modifying monomer in COPET.

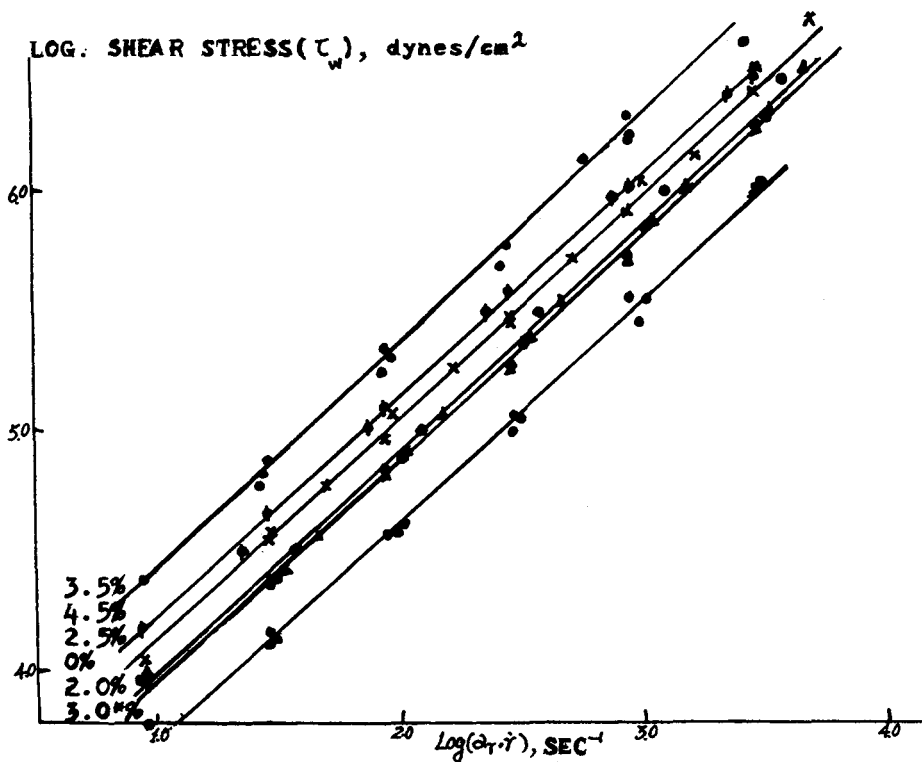


Fig. 5. Flow curves for COPET of different contents of modifying monomer (reference temperature, 285°C).

2.5, and 3.5 mol % and PET are 28.45, 31.02, 35.08, and 22.52 kcal/mol, respectively.

It is clear, as shown in Figure 4, that the viscous flow activation energy is a linear function of modifying monomer contents, which can be given by

$$E = 22.36 + 3.071 \times C$$

This shows that as the monomer content increases, the viscous flow activation energy increases linearly. Because the activation energy represents the mobility of molecular segments, sodium 3,5—di(carbonethoxy)benzenesulfonate in macromolecular chains restrains the motion of copolyester molecular segments.

Figure 5 shows flow curves of COPET melts for the temperature superposition. Data points for all three temperatures fall on smooth curves at all content levels investigated. Over shear rates range from 10 to  $10^4 \text{ s}^{-1}$ , the flow behavior of COPET is nearly Newtonian, that is, the curves are all straight lines with slopes of about 1. But there is a slight departure as modifying monomer content increases. The slopes of 0.9706, 0.9425, 0.9556, 0.9501, 0.9326, and 0.9276 result, relating to COPET for monomer contents of 0 (PET), 1.5, 2.0, 2.5, 3.5, and 4.5 mol %. So the flow behavior of COPET is slightly pseudoplastic with the increase of modifying monomer.

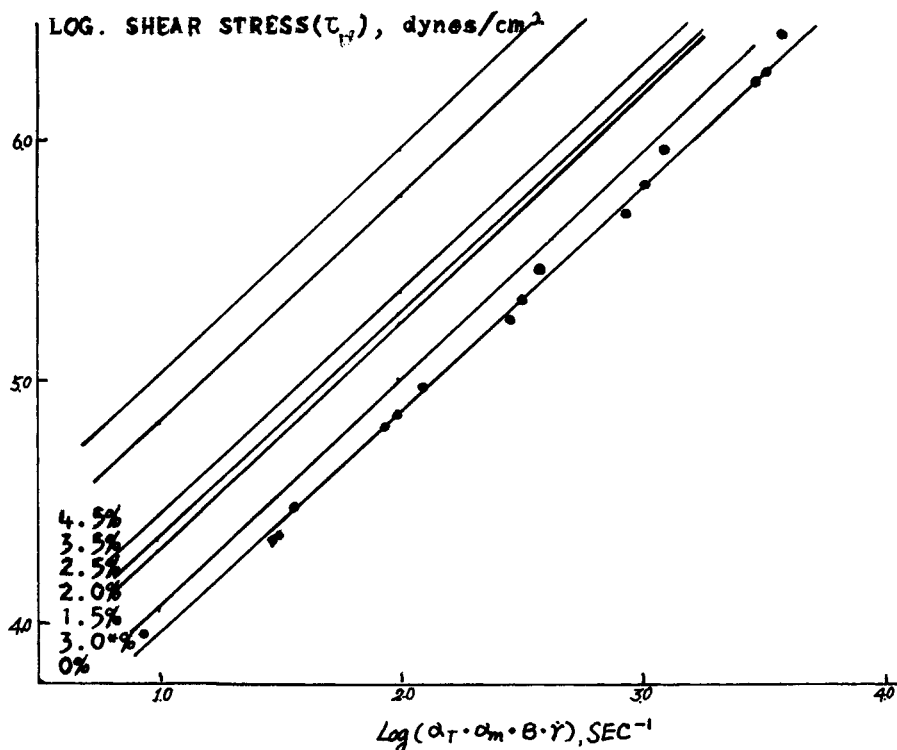


Fig. 6. Master curves (superposition of temperature, melting point, and molecular weight) for COPET of different modifying monomer contents. Reference temperature, 21°C + melting point; reference inherent viscosity, 0.652.

### Melt Viscosity and Modifying Monomer Contents

Because of different polymerization conditions, COPET chips possess different melting points and different inherent viscosities (Table I). They also affect melt viscosity in addition to modifying monomer content. By means of temperature superposition and molecular weight superposition,<sup>3</sup> we can determine the effect. In this study, one temperature, which was just 21°C higher than the melting point of each chip, and one inherent viscosity, which was the inherent viscosity of PET, were chosen as comparison bases. All data were shifted by melting point shift factor ( $a_m$ ) and inherent viscosity shift factor ( $B_w$ ) given by following two equations:

$$\ln a_m = A + B/T$$

and

$$B_w = (0.652/[\eta])^{5.1453}$$

where  $A$  and  $B$  are constants, which can be obtained by temperature shift factor  $a_T$ , and 0.652 is the inherent viscosity of PET.

The master flow curves were obtained, shown in Figure 6. As can be seen, shear stresses or melt viscosities of COPET increase with modifying monomer



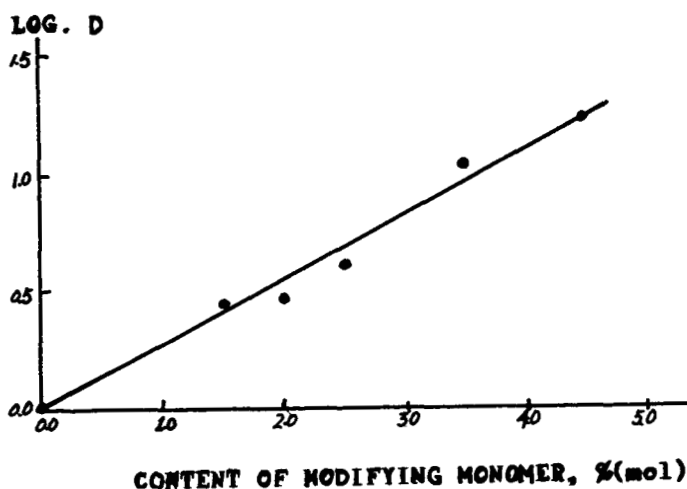


Fig. 7. Log of content shift factor as a function of contents of modifying monomer in COPET.

contents. The parallelism of curves in Figure 6 also suggests the possibility of modifying monomer content superposition. A technique similar to that used for temperature superposition was used successfully for the content superposition. The content shift factor ( $D$ ) was the ratio of the shear rate for one reference master flow curve to the shear rate for each of other flow curves at

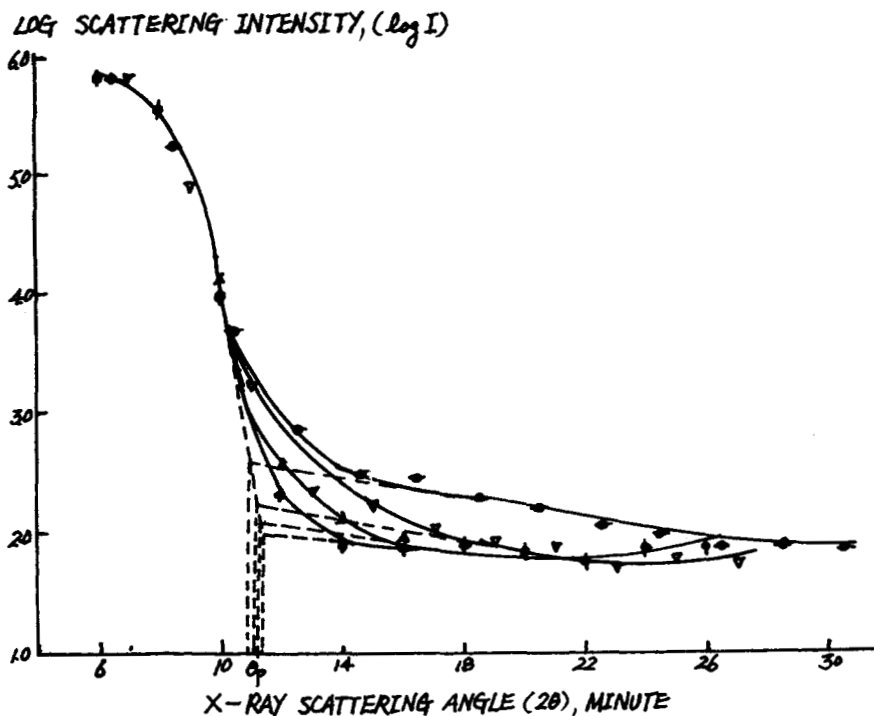


Fig. 8. Log  $I$  curves for COPET of different contents of modifying monomer in phenol/tetrachloroethane (1:1), 0.5% C. (—●—) 4.5%; (—▽—) 0%; (—△—) 1.5%; (—◐—) 3.5%.

constant shear stress defined as

$$D = (\dot{\gamma}_{re}/\dot{\gamma})_{\tau} = (\eta/\eta_{re})_{\tau}$$

The flow curve for PET was chosen as the reference curve. It is shown in Figure 7, the logarithm value of  $D$  is a linear function of contents, given by the linear regression equation as follows:

$$\log D = -0.0273 + 0.2825 \times C$$

So the melt viscosity as a function of modifying monomer content was given by

$$\log \eta = -0.0273 + 0.2825 \times C + \log \eta_{re}$$

This shows that the melt viscosity of COPET equals the melt viscosity of PET plus an extra by adding modifying monomer at the same melting point and inherent viscosity to PET.

How does this happen? In the dilute solution of COPET, concentration 0.5%, we studied the chain rigidity by the means of SAXS. The logarithm scattering intensity vs. scattering angle is plotted in Figure 8. The persistence length ( $L_p$ ) of PET, 1.5, 3.5, and 4.5 mol % monomer COPET are 169, 166, 163, and 173 Å, calculated by the Kratky equation as stated before. The static state flexibility ( $F$ ) of molecular chains was calculated in order to find the chain rigidity by the following equation:

$$F = L_p/N$$

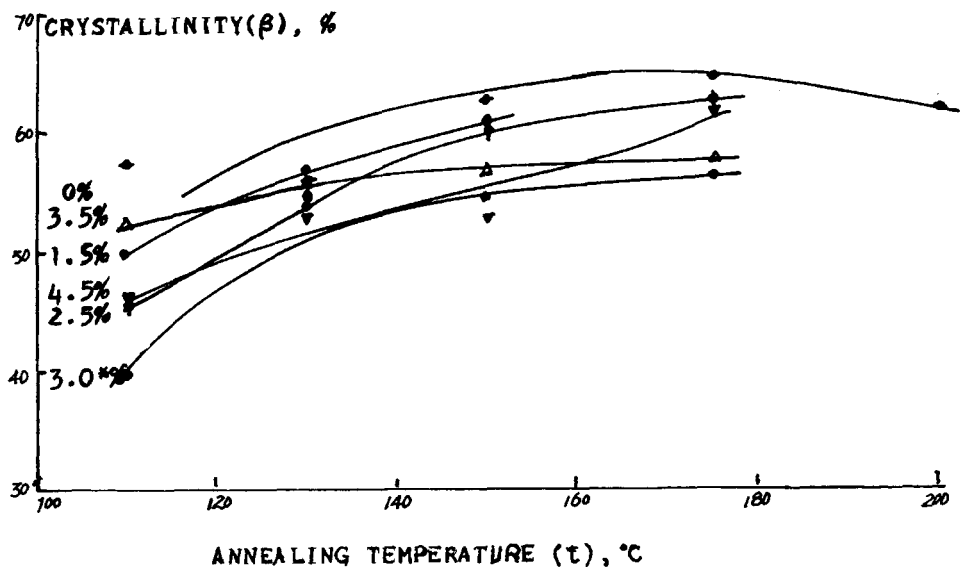


Fig. 9. Relation between annealing temperature and crystallinity of COPET fibers of different contents of modifying monomer.

where  $N$  is molecular length, given by

$$N = P \times M/U$$

where  $P$  is the identical period of *trans* configuration of COPET, taken as 10.75 Å;  $U$ , the molecular weight of structure unit of COPET, taken as 192;  $M$ , the molecular weight, calculated by inherent viscosity

$$M = ([\eta] \times 10^4 / 2.10)^{1/0.823}$$

The  $F$  values of PET, 1.5, 3.5, and 4.5 mol % monomer COPET are 0.184,

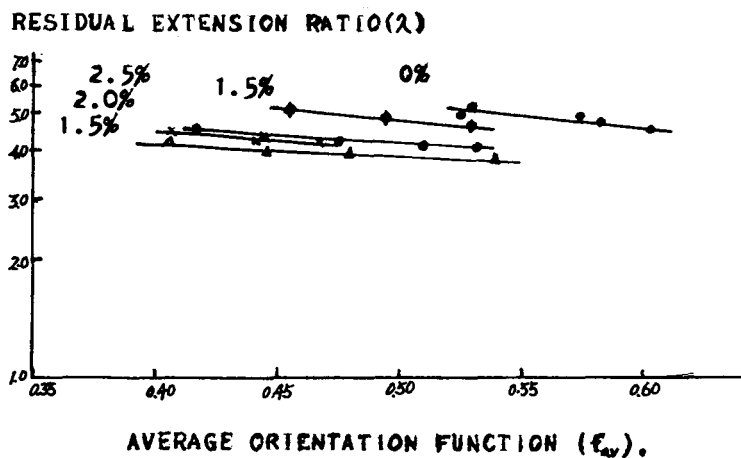


Fig. 10. Residual extension ratio as a function of average orientation function of COPET fibers. (6%, in oil).

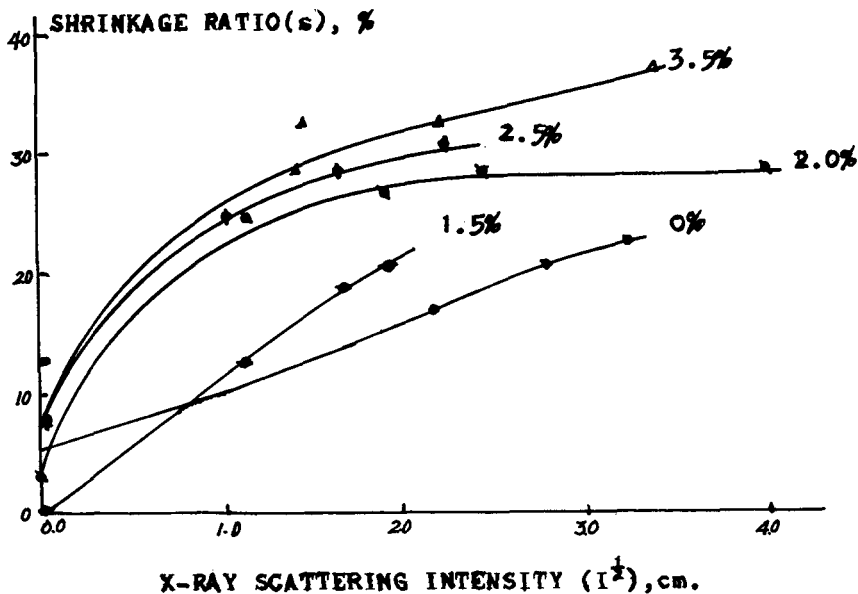


Fig. 11. Shrinkage ratio as a function of scattering intensity of COPET fibers.

0.228, 0.250, and 0.329, increasing with monomer contents. The bigger the  $F$  is, the stronger the chain rigidity will be. So the increase in chain rigidity causes the increase in melt viscosity of COPET.

### Fiber Properties

The crystallinity of COPET fiber was studied by X-ray diffraction. Because Na 3,5—di(carbonethoxy)benzenesulfonate in molecular chains of COPET cannot enter the crystalline region, the crystallinities of COPET fibers decrease with the increase of monomer contents, as shown in Figure 9. This can be proved by the unchanged diffracting angles of (010), (110), and (100) reflecting planes, which are 17.8°, 23.0°, and 25.9° for all testing fibers.

As annealing temperature increased, the shrinkage ratio of COPET fibers increased, and the residual extension ratio decreased. The effects of temperature on orientation functions, that is, crystalline orientation function and amorphous orientation function, are different. But the average orientation function increases with the temperature, shown in Figure 10. It is also shown that the average orientation function ( $f_{av}$ ) decreases as the monomer content increases.

The crystalline and amorphous region of COPET fibers were studied by SAXS. Scattering intensities decrease with the increase of monomer contents at the same shrinkage ratio, shown in Figure 11. This means that the difference of electron density between the crystalline region and the amorphous region is less in COPET fibers than in PET fiber.

The long period of COPET fibers decreases with the increase of monomer contents at the same shrinkage ratio, shown in Figure 12. So, as shown in

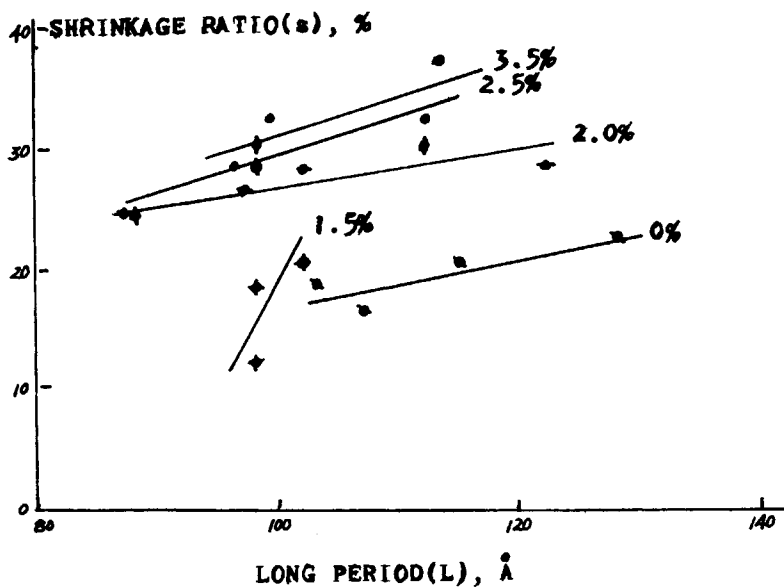


Fig. 12. Shrinkage ratio as a function of long period of COPET fibers.

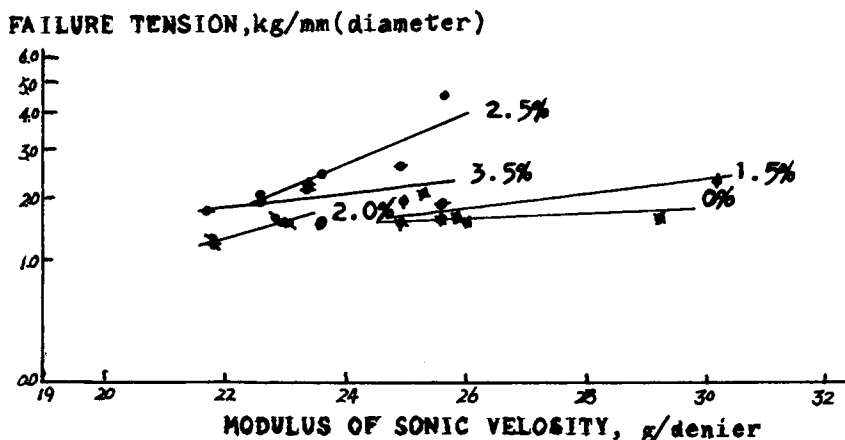


Fig. 13. Relation between failure tension and modulus sonic velocity.

Figures 11 and 12, since the increase of annealing temperature results in the increase of the long period and the difference of electron density between the crystalline and the amorphous region, the structure of the crystalline and amorphous regions becomes more different in COPET fibers as the temperature increases.

The relation between failure tension and modulus of sonic velocity of COPET fiber is shown in Figure 13. With the increase of sonic velocity, the failure tension of COPET fiber increases. With the increase of monomer content, the failure tension of COPET fiber tends to increase at the same sonic velocity of fiber.

### CONCLUSION

In this paper, the flow behavior and fiber structure of COPET have been studied. Three main points have been discussed: (1) the flow curves of COPET both experimental and superpositioned; (2) the effect of modifying monomer content on viscous flow activation energy and melt viscosity; (3) the effect of the monomer content on the crystallinity, orientation function, long period, SAXS intensity, and failure tension of COPET fibers. The increase of melt viscosity of COPET and the decrease of crystallinity and the orientation and residual extension ratio (larger fiber shrinkage ratio) of COPET fibers, all these can be explained by the increase of viscous flow activation energy and the rigidity of molecular chains of COPET. It has been shown that in order to overcome difficulties during spinning and processing of COPET fibers the inherent viscosity of COPET requires an adequate decrease.

The authors wish to thank Mr. Yang Zhonghe and Mr. Liu Hanxing for their help during this work.

### References

1. Bri. Pat., 826,248; U.S. Pat., 3,185,671; Ger. Pat., 1,959,436; Jpn. Pats., 73 95, 495; 75 42, 199; 76 32, 823; 80 98, 966; 81 118, 925; 82 11, 232.

2. D. R. Gregory, *J. Polym. Sci., Part C*, **30**, 399-406 (1970).
3. D. R. Gregory, *J. Polym. Sci.*, **16**, 1479-1487 (1972).
4. *Trans. Soc. Rheol.*, **17**(1), 191-195 (1973).
5. Edwin Boudreaux, J., and John A. Cuculo, *J. Appl. Polym. Sci.*, **27**, 301-318 (1982).
6. R. J. Samuels, *Structured Polymer Properties*, Wiley, New York, 1974.
7. He-cheng Xian-wei Tong-xun (Chinese), **3**, 53 (1976).
8. O. Kratky, *Pure Appl. Chem.*, **12**, 483 (1966).
9. He Manjun, *Macromolecular Physics*, Fu Dan Univ., Shanghai, 1982.

Received May 22, 1986

Accepted August 29, 1986